ELSEVIER

Contents lists available at ScienceDirect

Journal of Membrane Science

journal homepage: www.elsevier.com/locate/memsci





How alginate monomers contribute to organic fouling on polyamide membrane surfaces?

Yuan Xiang, Rong-Guang Xu, Yongsheng Leng

Department of Mechanical & Aerospace Engineering, The George Washington University, Washington DC, 20052, United States

ARTICLE INFO

Keywords:
Membrane fouling
Polyamide
Alginate
Molecular dynamics
Water treatment

ABSTRACT

Organic fouling of polyamide membrane surfaces with alginate molecules in an aqueous solution is studied through computer molecular simulations. Here, we focus on the molecular binding properties of β -D-mannuronic acid (M) and α -L-guluronic acid (G) alginate monomers on a polyamide membrane surface. Free energy calculations show that M alginate monomers exhibit significant hydrophobic attractions with certain types of benzene ring units in a polyamide chain, though such hydrophobic interactions are not as strong as the ionic bridge binding between the M monomer and the carboxylate group on a polyamide membrane surface. This is in contrast to the fouling behavior of G alginate monomers to which such hydrophobic interactions with a membrane surface do not exist, and the organic fouling is largely attributed to the ionic bridge binding between the G monomer and polyamide carboxylate groups mediated by divalent metal ions. Molecular dynamics simulations of different alginate oligomers near a polyamide surface show that hydrophobic interactions between the M-containing oligomers and polyamide membrane surface result in a much shorter pathway of fouling than that of pure G-oligomers. These hydrophobic interactions, together with the mobility of M monomers on a polyamide chain surface, further reduce the docking time of M-containing oligomers compared to pure G-oligomers, and thus enhance the surface fouling.

1. Introduction

Polyamide membrane has been widely used in water treatment, especially during seawater desalination and wastewater reclamation by membrane separations [1–3] as a reverse osmosis/nanofiltration (RO/NF) membrane [4–7]. However, membrane separation suffers the fouling problem [5,8,9], especially organic fouling in which organic species accumulate onto membrane surfaces that impacts the separation efficiency. Developing highly efficient antifouling membranes needs a better understanding of the foulant-polyamide molecular interactions. From this fundamental aspect, computer molecular simulations can play a critical role [5,8–13]. Many theoretical investigations using molecular dynamics (MD) simulations contributed significantly to the understanding of water transport in membranes and ion rejection during membrane separations [14–28]. Very recently, computer molecular simulations have been employed to study the organic fouling of RO/NF membranes [29–32].

Finding the highly possible fouling locations on a membrane surface is still facing many challenges. This is largely due to the complexity of the chemistry and morphology of the membrane surface. Free energy calculations to search for the binding sites that have high fouling potentials can provide molecular insights into the foulant-membrane interactions [32]. In this study, we focus on molecular interactions between different building blocks of polyamide membrane and alginate monomers. Polyamide is selected as a semi-permeable model membrane because it is widely used in industry and has been studied extensively in both experiments [1–3] and computer molecular simulations [30,31, 33–39]. Alginate is selected as a foulant model because it widely exists in the environment and is one of the major contributors to organic fouling [40–42].

In our recent MD simulation studies [30,31], we showed that divalent metal ions can form very strong ionic binding between alginate molecules and polyamide membrane surface, largely in the form of ionic bridges that may take different molecular binding conformations and strengths. In the present study, in addition to ionic binding, we turn to other possible molecular binding conformations that may contribute to the organic fouling. Our motivation is based on the following two aspects. First, it has been shown that membrane fouling occurs not only in

E-mail address: leng@gwu.edu (Y. Leng).

^{*} Corresponding author.

neutral or basic aqueous solutions, but also in an acidic environment [43]. When carboxylate functional groups on the membrane surface are protonated in an acidic solution, ionic bridges are usually not easy to form. Second, in our previous simulation studies [30,31], we only considered alginates consisting of L-guluronic acid monomers because they tend to form alginate gels [44,45]. In this work, we will study both L-guluronic and D-mannuronic acid monomers (L and D are named after Latin *laevus* and *dexter*, meaning *left* and *right*) [46]. The latter also takes a large portion of alginate population in the environment. Our simulation results show that the D-mannuronic acid monomers play an even more important role than the L-guluronic acid monomers in the initial stage of organic fouling.

In section 2, we first introduce a hybrid method to build an amorphous polyamide membrane surface that can properly represent polyamide surface chemistry. Simulation results are presented and discussed in section 3, followed by our summary and further discussions in section 4

2. Computer molecular simulations

2.1. Molecular models

2.1.1. Polyamide membrane

Polyamide membrane, the widely used RO/NF membrane material for desalination and water purification in industry, is made from the polymerization of m-phenylenediamine (MPD, Fig. 1a) and trimesoyl chloride (TMC, also called benzene-1,3,5-tricarbonyl chloride, Fig. 1b). During the polymerization process, the acyl chloride groups in TMC (-COCl) react with amine groups in MPD (-NH₂) to form amide bonds (-CONH–) (Fig. 1c). The complexity of polyamide structure originates from its monomer structure. MPD has two amine groups (-NH₂) and TMC has three acyl chloride groups (-COCl). Therefore, some TMC molecules react with three MPDs (molecule A in Fig. 1c), while others react with only two or less (molecule B in Fig. 1c), resulting in complex cross-linked structure. The survived acyl chloride groups (-COCl) in TMC will eventually hydrolyzed to form carboxylate groups (-COO¹, Fig. 1c in pink) which are negatively charged.

As far as we know, there are three typical methods to build polyamide block to reflect the cross-linked structural feature of the membrane. The first method was proposed by Kotelyanskii et al. [36,37] with some later revisions by others. In this method, chain structures with alternate MPD and TMC monomers are built (Fig. 2a). In order to make a

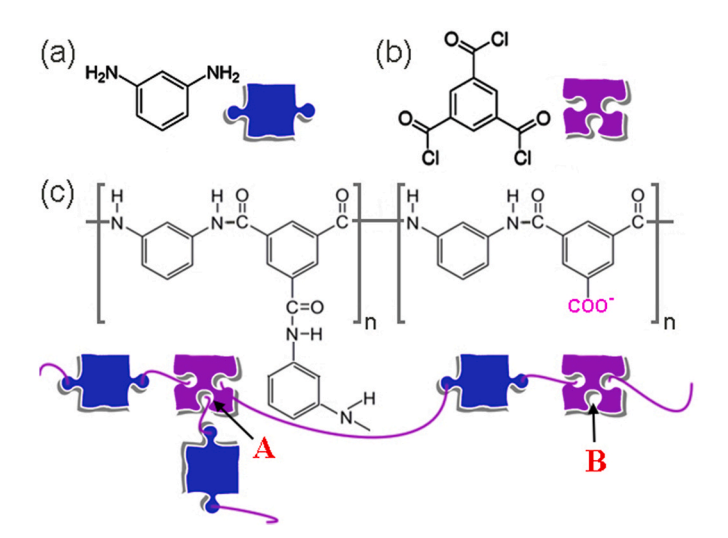


Fig. 1. Two molecular units in polyamide: (a) m-phenylenediamine (MPD) and (b) trimesoyl chloride (TMC). (c) Repeated dimeric unit in a polyamide chain. The TMC molecule marking as "A" reacts with three MPDs, while the TMC molecule marking as "B" reacts with only two MPDs.

cross-linked structure, a post-processing stage is introduced, in which extra MPD molecules are added to the simulation system. Cross linking is realized by bridging carboxylic groups separated by no more than 7 ± 2 Å with a bifunctional MPD monomer (the so-called *distance heuristic method*, see Fig. 2a the red dashed lines). One of the advantages of this protocol is that chain conformations are generated with the correct Boltzmann weight. This strategy is recently adopted by Hughes et al. [32,35] and our research group [30,31,47].

The second method was proposed by Harder et al. [34] The building blocks in the polymer model are individual MPD and TMC monomers (Fig. 2b). These monomers are first randomly inserted into a large MD simulation box, followed by NPT MD equilibrium runs to reach the experimental density of the membrane (~1.38 g/cm³) [48,49]. All amide bonds are introduced based on a *distance heuristic method*. If the distance between TMC and MPD is less than 3.25 Å, the amide covalent bond will be set (Fig. 2b the black solid lines). The membrane structure built by the Harder's method is intrinsically cross-linked.

Ridgway et al. proposed the third method of building polyamide membrane blocks [39,50]. Here, MPD and TMC monomers are alternately introduced uniformly into a cubic lattice (Fig. 3). Random walks through the monomer matrix to build MPD-TMC amide bonds are performed, creating randomly folded self-avoiding polymer chains (Fig. 3, the purple and green pathways). After completion of the polymer chain, search for any chain-resident TMC monomer pairs that remain separated by a common as-yet non-bond MPD monomers is performed (see Fig. 3 the two blue arrows pointing to a common MPD). Then a probability function is introduced to determinate whether a cross-linked structure is formed there.

The three methods discussed above have their own advantages and disadvantages. In this study, we consider a hybrid approach to build a polyamide membrane model by taking advantage of the three methods. Our motivation to develop this hybrid method has two considerations. First, the method should be able to adapt to several key experimentally characterized surface properties, such as surface charge density, functional group density, and the degree of cross-linking. Second, the method can be easily used to control some surface properties to identify the relationship between a specific surface characterization and its surface fouling property. Our hybrid method consists of two major steps: the first step is to build a polyamide surface model with the desired surface charge density and functional group distributions; the second step is to build the remaining bulk polyamide membrane with the designed cross-linking ratio.

To build a membrane surface with a desired surface charge density, we first use the modified Ridgway's approach [39,50]. As shown in Fig. 4a, TMC and MPD monomers are uniformly distributed on a surface. We can control the local surface to be highly negatively charged by removing all MPD monomers on the surface, leaving only carboxylate groups (-COO) derived from hydrolyzed TMC monomers (Fig. 4b). Alternatively, we can remove all TMC monomers in the surface, generating a neutral surface exposing only MPD monomers (Fig. 4c). In order to connect all the monomers on the surface to the bulk part, a random walk will be performed starting from the surface monomers and ending at the bulk-surface interface (Fig. 4d). With this modified method, we can essentially build any surface models with the desired surface charge densities and functional group distributions. In the second step, starting from the end units of the interfacial chains, as shown in Fig. 4d, we use Kotelyanskii's method [36,37] to build polyamide bulk membrane according to proper Boltzmann weight. The membrane model built using the hybrid method should match the chemical composition, the membrane density, and the cross-linking ratio characterized by experiments.

The hybrid method which separates the surface model from the bulk membrane has the following two advantages: First, the surface properties such as the surface charge density and functional group distributions are controllable. Therefore, we can build representative model membrane surfaces, identifying and validating some critical fouling mechanisms. Such an example surface will be studied in section 3.3. Second,

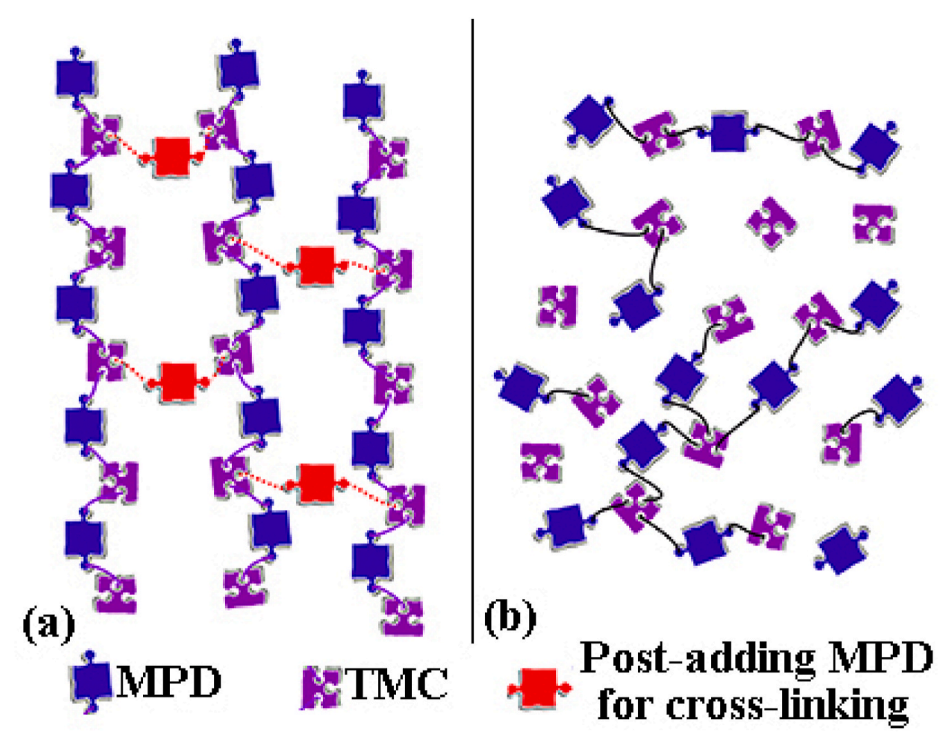


Fig. 2. Schematic of different polyamide membrane models. (a) Kotelyanskii's method with modifications. Purple solid lines show the pre-built amide bonds. Red dashed lines represent amide bonds formed by distance heuristic; (b) Harder's method. All amide bonds are formed according to distance heuristic, illustrated by black solid lines. (For interpretation of the references to color in this figure legend, the reader is referred to the Web version of this article.)

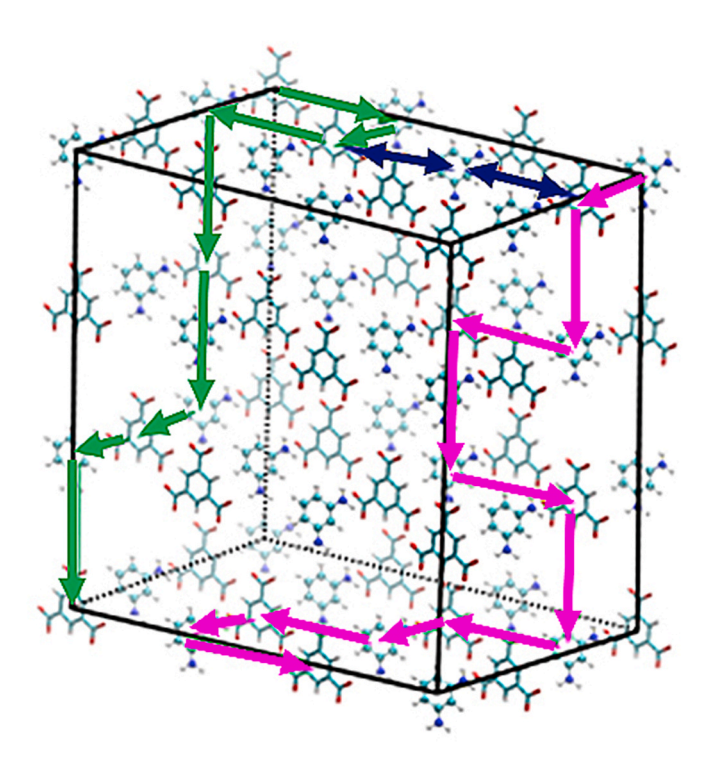


Fig. 3. Ridgway's method with random walk in a cubic 3D lattice uniformly filled with MPD and TMC monomers. The purple and green pathways represent two polymer chains. The blue arrows show the formation of a cross-linked structure. Colors: red, O; white, H; light blue, C; dark blue, N. (For interpretation of the references to color in this figure legend, the reader is referred to the Web version of this article.)

some unfavorable local structures with very high energies due to the cross-linking heuristic method [36,37] will be avoided, resulting in more realistic surface structures.

Polyamide surface model is built based on experimentally characterized surface charge densities, yielding the surface densities of carboxylate and amine groups around 0.4 M and 0.04 M, respectively. These values are close to the experimentally characterized densities of 0.432 M [51] and 0.036 M [52], respectively. To build the bulk polyamide membrane, a total of 20 polyamide chain molecules are folded into the simulation box with each chain molecule containing ten repeated MPD-TMC units (Fig. 2a). MPD monomers are then inserted to create crosslinked polyamide membrane (Fig. 2a). A total of 7020 water molecules are added to the simulation system to hydrate the amorphous polyamide membrane, whose dimensions are around 72 Å \times 36 Å \times 38 Å. A total of 92 sodium ions are added to the system to compensate the charged sites in polyamide membrane. Moreover, when studying ionic bridge binding between alginate and polyamide membrane, 12 divalent Ca²⁺ ions and 24 Cl⁻ co-ions are also added to the simulation system (equivalent to ~ 0.1 M CaCl₂ solution). A vapor phase is maintained above the water-polyamide complex, allowing the system pressure to be comparable to the water vapor pressure [53,54].

Upon the completion of the MD equilibrium run of 10 ns, the bulk membrane density and the degree of cross-linking are found to be around $1.36~\text{g/cm}^3$ and 43%, respectively. These results are consistent with previous experiments and theoretical calculations [34,35,37]. [55].

2.1.2Alginate foulant

Alginates are linear polymer chains consisting of β -D-(1 \rightarrow 4)-mannuronic acid (M, Fig. 5a) and α -L-(1 \rightarrow 4)-guluronic acid (G, Fig. 5b) monomers. Fig. 5c and d shows the molecular configurations of M and G alginate monomers in hydration state. In the present study, we mainly focus on molecular interactions between polyamide chains with individual G/M monomers, followed by further investigations between polyamide membrane and alginate oligomers containing multiple G/M

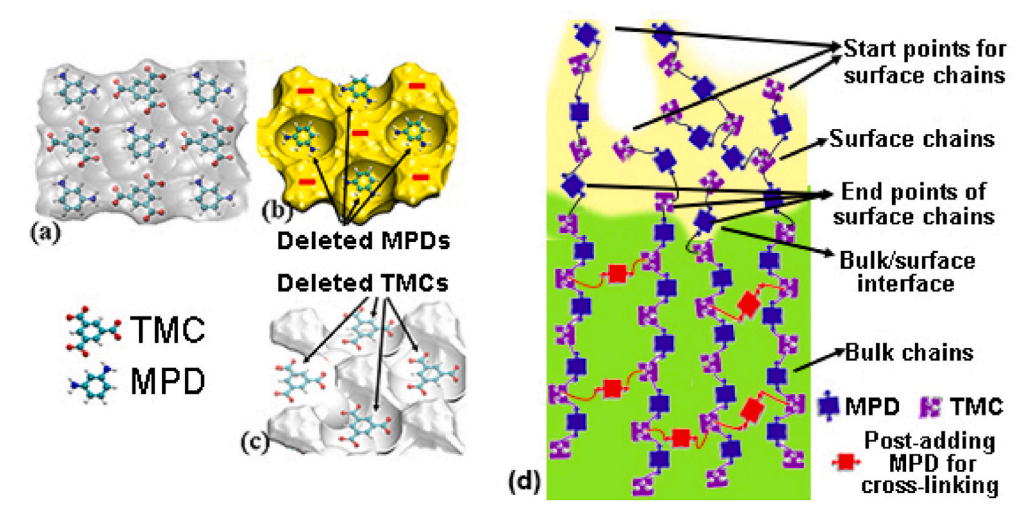


Fig. 4. Building a membrane surface with a desired surface charge/functional group densities by the modified Ridgway's approach. Surfaces are represented by the van der Waals contours. (a) The uniformly distributed TMC and MPD monomers on a surface; (b) Controlling the local surface charge density to obtain a highly negatively charged surface by removing the nearby MPD monomers on the surface; (c) obtaining a regional neutral surface by removing the nearby TMC monomers on the surface; (d) Schematic of the hybrid method in which only polyamide chains that connect the surface and the bulk regions are shown. Colors: red, O; white, H; light blue, C; dark blue, N. (For interpretation of the references to color in this figure legend, the reader is referred to the Web version of this article.)

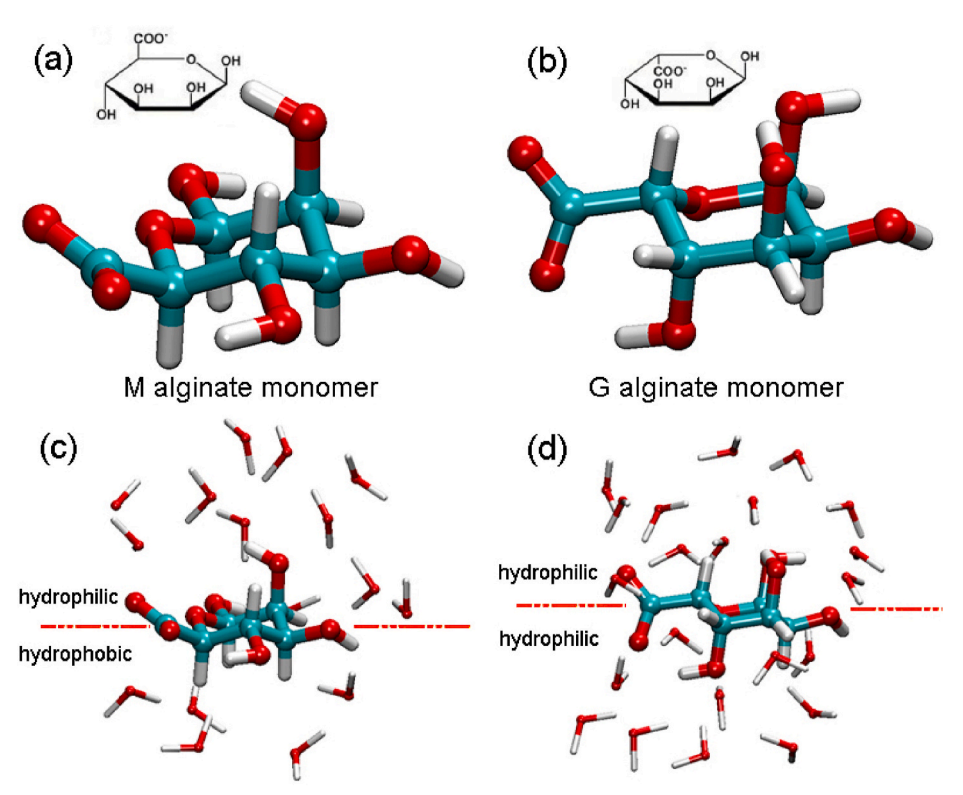


Fig. 5. Molecular configurations of (a) the deprotonated M and (b) the deprotonated G alginate monomers. The chemical structural formula of each monomer is shown at the top of each panel. Panel (c) and (d) show the coordinated water molecules around the deprotonated M and the deprotonated G alginate monomers in hydration state, respectively. Colors: red, O; white, H; light blue, C. (For interpretation of the references to color in this figure legend, the reader is referred to the Web version of this article.)

monomers. Previously, it was reported that alginates with only G monomers have specific spacing and geometry of the carboxylate functional groups for cation binding [44]. The strong interactions between the divalent ions and G monomers lead to the association of chains to form alginate gel, which is believed to be one of the main contributors to organic fouling [45]. In the present work, we show that the M monomers can have more complex molecular interactions with polyamide chains than the G monomers. Considering the acid-dissociation-constant (pKa) of alginic acid being usually around 3.38–3.65 [56,57], we anticipate that in the neutral environment (pH \sim 7) all carboxyl groups in alginates are deprotonated [57]. Therefore, in our simulation system, one sodium ion (Na $^+$) for each deprotonated -COO $^-$ site is introduced to balance the negative charge site.

2.2. Computer simulations

2.2.1Force field and simulation system

All simulations are performed using the LAMMPS computational package [58]. We use the particle—particle particle—mesh solver to calculate the long-range electrostatic interactions [59]. Periodic boundary conditions are applied in three dimensions. The cutoff distance for the short-range Lennard-Jones interactions is set to 10 Å. The temperature is controlled at 296 K by the Nosé—Hoover thermostat [60]. The equations of motion of the particles are propagated through the velocity Verlet algorithm with a time step of 1 fs in a constant-NVT ensemble. We use the consistent valence force field (CVFF) [61] to describe the interatomic interactions between all atoms, as implemented in our previous work [30]. Atomic partial charges for polyamide and alginate molecules are recalibrated by using quantum mechanical

density functional theory calculations with the B3LYP/6-31G** functional/basis set and by the CHarges from ELectrostatic Potentials using a Grid (CHELPG)-based method [62]. We use the flexible simple-point charge (SPC) model for water in the simulations^{39, 40}, which is compatible with the CVFF force field parameters. We also applied the OPLS [63,64] force field to check against the CVFF for the purpose of verification of simulation results. The two force fields give similar free energy values, thus, only the results from the CVFF are reported in this work. The Aqvist SPC-compatible ion potential parameters [65] for Na⁺ and Ca²⁺ ions are employed in our simulations. For halide Cl⁻ anion, we use the potential parameters developed by Joung et al. [66].

2.2.2Free energy calculations

The umbrella sampling method [67,68] is used for free-energy calculations between alginate molecules and polyamide chain units. The free energy profile is calculated by $G(d) = -k_BT \ln[P(d)]$, where k_B is the Boltzmann's constant, T is the temperature, and P(d) is the probability distribution of molecular sampling distance d, between the alginate molecule and a specific polyamide chain unit. The total sampling distance d, is divided into N independent simulation segments. In each segment i, a constrained umbrella potential is applied to the system to obtain a biased probability distribution $P(d_i)$. The unbiased distribution P(d), is then reconstructed through the histogram reweighting method [67,68] for the free energy calculations. The approach allows one to obtain the equilibrium free energy of the system. During the umbrella sampling, a total of N = 40 succeeding sampling intervals are arranged within the distance of d = 3-13 Å, giving a sampling interval of 0.25 Å in which a harmonic spring with a spring constant of 2 kcal/(mol \mathring{A}^2) is used. Molecular conformations are sampled by gradually changing the sampling distance by the spring. In each sampling interval, an equilibrium MD simulation run of at least 4 ns is performed to statistically sample the molecular conformations.

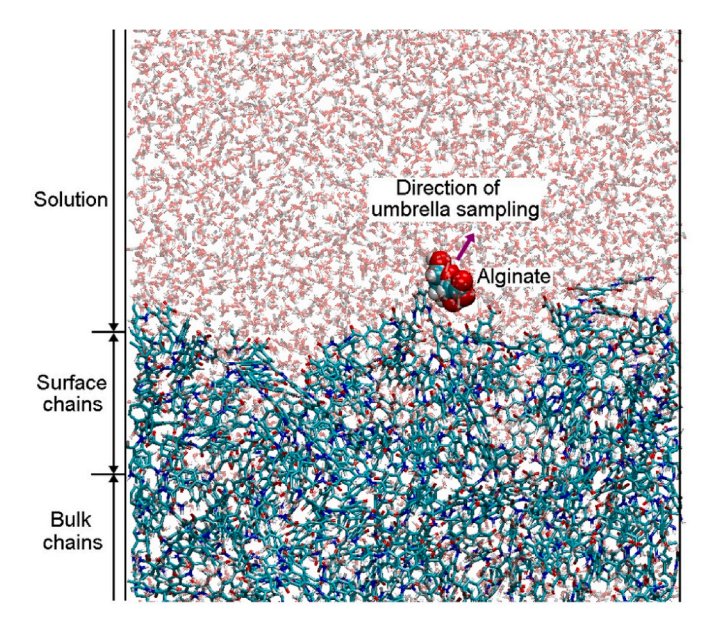


Fig. 6. Snapshot of a typical docking conformation of an M alginate monomer on a polyamide membrane surface. The alginate monomer is represented by its van der Waals contour. Colors: red, O; white, H; light blue, C; dark blue, N. (For interpretation of the references to color in this figure legend, the reader is referred to the Web version of this article.)

3. Simulation results

3.1. Interactions between individual alginate monomers and polyamide chain units on a membrane surface

Fig. 6 shows a typical docking conformation of an M alginate monomer on a polyamide membrane surface, which is built using the hybrid method discussed in section 2.1.1. Because alginate molecules contain both carboxylate and hydroxyl groups, they are usually considered as hydrophilic. However, recent studies showed that alginates can also have a strong binding with hydrophobic membrane surfaces such as polypropylene [69]. While it is known that a hydrophilic alginate molecule can form strong ionic bridge binding with a polyamide membrane surface [30,31], its strong interaction with hydrophobic surfaces is somewhat surprising. Stewart et al. found that alginates containing M monomers exhibit a hydrophobic behavior and could deposit to the hydrophobic polypropylene membrane surfaces [69]. Considering benzene rings in a typical polyamide chain molecule on the membrane surface are possible hydrophobic groups, we are particularly interested in the molecular interactions between the M alginate monomer and different benzene ring units in a polyamide chain on the surface.

To understand why the M alginate monomer shows both hydrophilic and hydrophobic (amphiphilic) behaviors, we now consider its equilibrium molecular structure as shown in Fig. 5a. The downside of the M monomer contains three non-polar hydrogen atoms which likely form a hydrophobic side. The four hydrophilic hydroxyl groups of the M monomer either lie flat or stand upward. Such an amphiphilic property – the combination of hydrophobic downside and hydrophilic upside, is a unique structural feature in the M monomer. For comparison, the G monomer shown in Fig. 5b has hydroxyl groups on both sides, indicating that very likely the G monomer will be hydrophilic on both sides. In Fig. 5c and d, we show the coordinated hydration water molecules around the deprotonated M and G alginate monomers, respectively. Direct counting the number of coordinated water molecules on both sides show that there are much less coordinated water molecules on the hydrophobic side (about 4-6) than that on the hydrophilic side (about 10–14) for the M monomer (see Supplementary Information section S1), demonstrating the amphiphilic structural feature of the M monomer. In contrast, the number of coordinated water molecules on both sides of the G monomer are almost equal (about 10–15), indicating that both sides of the G monomer are hydrophilic.

To provide further insights into the hydrophobic behavior of the M monomer due to its hydrophobic/hydrophilic structural segregation, we use umbrella sampling [67,68] to calculate the free energy profiles between an M monomer and different benzene ring units on a polyamide membrane surface. After structural analyses on the chemistry of different benzene rings on the polyamide membrane surface, we have identified five different types of benzene ring units that are summarized in Table 1 and further illustrated in Fig. 7. These five benzene ring units provide possible hydrophobic sites on which umbrella sampling is performed to search for the free energy profile of the alginate monomer-polyamide benzene ring unit complex, as shown in Fig. 6.

We now first study the interactions between the M monomer and different benzene ring units on the polyamide chain surface. Here we choose each type of benzene ring unit from multiple different sites on the

 Table 1

 Classification of benzene ring units on a polyamide membrane surface.

Type	Chemistry environment
1	benzene ring connected to two carboxylate groups and one amide group
2	benzene ring connected to one carboxylate group and two amide groups
3	benzene ring connected to two amide groups
4	benzene ring connected to three amide groups
5	benzene ring connected to one amine group and one amide group

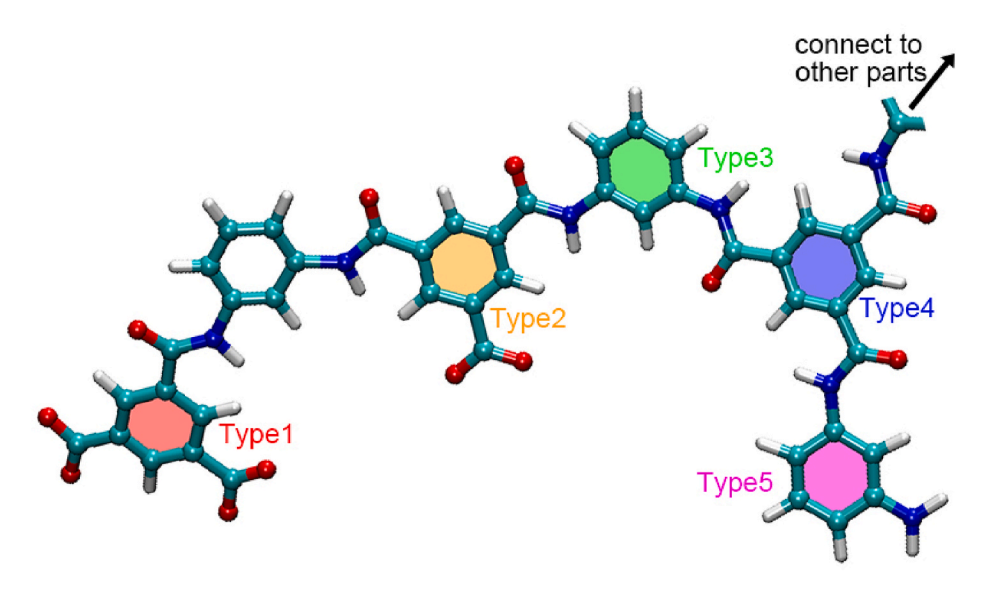


Fig. 7. Summary of five typical benzene ring units on a polyamide chain molecule. Atom colors: red, O; white, H; light blue, C; dark blue, N. (For interpretation of the references to color in this figure legend, the reader is referred to the Web version of this article.)

membrane surface to perform independent free energy calculations. Free energy curves corresponding to different types of benzene ring units are obtained by averaging over simulation results from different sites (see Supplementary Information section S2). Fig. 8a shows the free energy variations versus the distance d between the center-of-mass of the M alginate monomer and the center-of-mass of specific benzene ring unit. The free energy value at larger distance d = 7.5 Å is used as the reference point. It is interesting to see that interactions with different benzene ring units yield very different free energy profiles which can be broadly classified into two categories. Free energy curves corresponding to type 3, 4 and 5 benzene units show a global minimum about -2 kcal/mol at a distance close to d = 4 Å, while those relevant to type 1 and 2 benzene units only show a very shallow energy valley at about 4.5 Å, with a much less dissociation energy of 0.5 kcal/mol. Molecular binding conformations (Fig. 9a-c) clearly show that the hydrophobic side of the M monomer has a strong tendency to be in close contact with the type 3, 4 and 5 benzene units, signifying a strong hydrophobic attraction. Such a hydrophobic contact conformation is not seen in Fig. 9d for type 1 and 2 benzene contacts, in which the hydrophobic side of the M monomer faces a much random direction. It is interesting to see that the distance of the energy minimum for type 4 is slightly (0.2 Å) larger than those for type 3 and 5 in Fig. 8a. This is largely due to the different functional

groups connected to the benzene units. Specifically, the $-\mathrm{NH}$ and $-\mathrm{NH}_2$ -groups connected to type 3 and 5 benzene rings are electron-donating groups due to the resonance effect, while the $-\mathrm{CO}-$ groups connected to type 4 benzene rings are electron-withdrawing group. Therefore, the average partial charges of the benzene carbon atoms in type 3 or 5 benzene unit are slightly more negative (0.1e/atom) than those in type 4 benzene unit. As the electrostatic potential of the hydrophobic side of the M alginate monomer is slightly positive [69], the slightly larger electrostatic attraction between the hydrophobic side of the M alginate monomer and the type 3 or 5 benzene ring unit leads to slightly shorter equilibrium distance.

For comparison, in Fig. 8b we show the free energy profiles for the interactions between the G monomer and the five different benzene ring units in polyamide chains on the surface. Because the G alginate monomer does not have any hydrophobic side, all the free energy curves have very shallow valleys. The insignificant dissociation energies within 0.5 kcal/mol are largely attributed to the van der Waals interactions between the foulant monomer and the polyamide membrane surface.

Given the existence of a hydrophobic side of the M alginate monomer, its hydrophobic interaction with type 3, 4 and 5 benzene units in a polyamide chain should be correlated to the less hydration state of these three types of benzene rings. Fig. 10a shows the variations of the

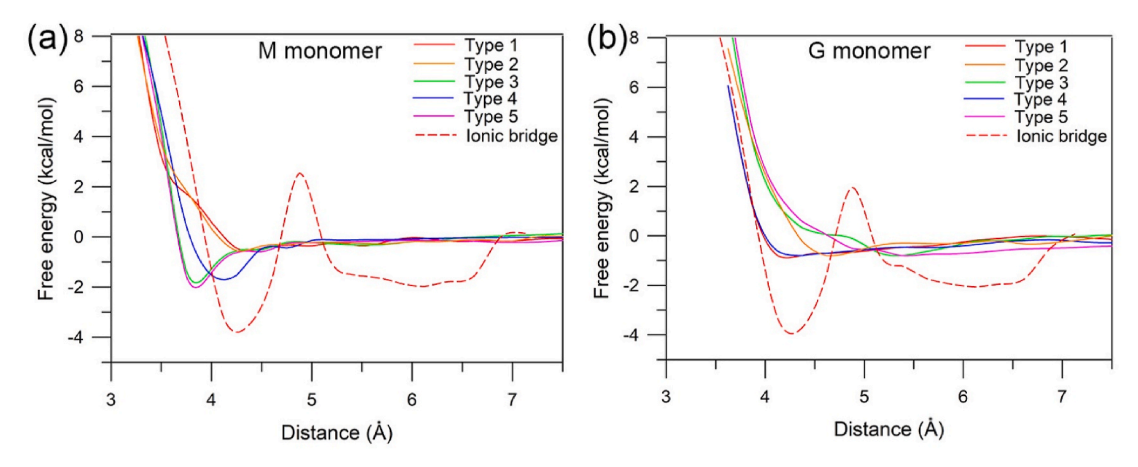


Fig. 8. Free energy profiles of (a) M alginate monomer and (b) G alginate monomer in contact with different types of benzene ring units in a polyamide chain molecule (solid lines). The red dashed line in (a) and (b) represents the ionic bridge binding between two carboxylate groups from the alginate monomer and the polyamide chain molecule. (For interpretation of the references to color in this figure legend, the reader is referred to the Web version of this article.)

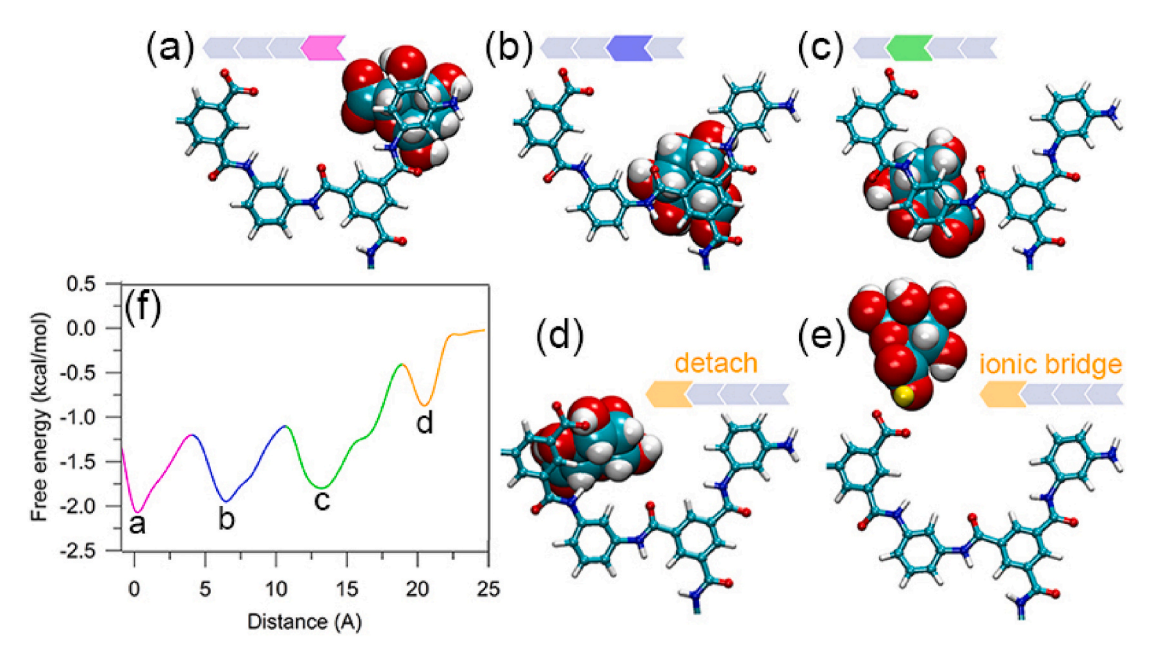


Fig. 9. (a)–(d): Metastable conformations of the M alginate monomer near each type of benzene units on a polyamide chain. (e) Ionic bridge binding between the monomer and the polyamide chain. (f) Variations of the free energy versus the distance s along the backbone of the polyamide chain, with the equilibrium position in (a) setting as distance s = 0. Points a - d in panel f correspond to the positions of metastable configurations, as shown in (a)–(d), respectively. Arrows with different colors in (a)–(d) correspond to different free energy segments in (f). Colors: red, O; white, H; light blue, C; dark blue, N; yellow, Ca²⁺ ion. (For interpretation of the references to color in this figure legend, the reader is referred to the Web version of this article.)

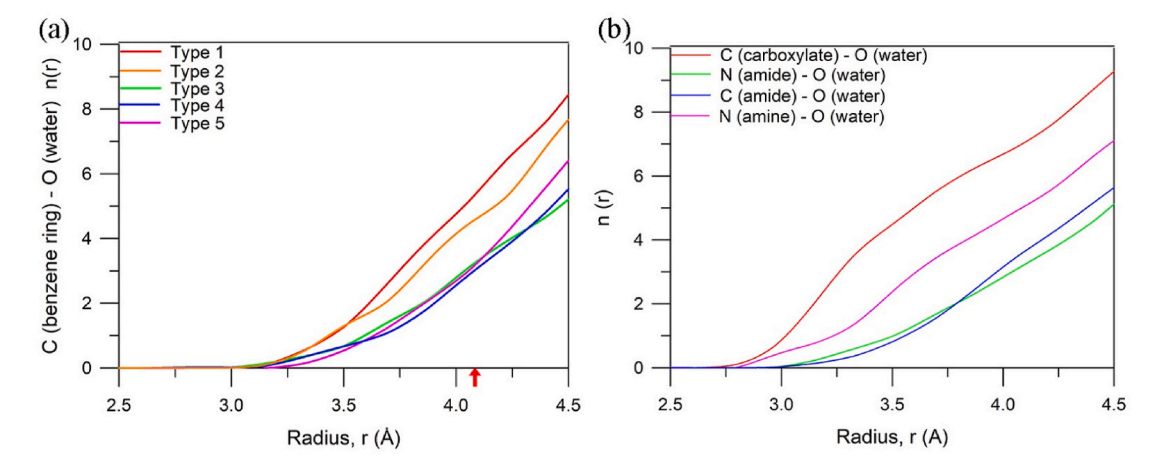


Fig. 10. (a) Average water coordination number around the carbon atoms in each type of benzene ring units in a surface polyamide chain. All the six constituent carbon atoms in each benzene ring are considered by calculating the average coordination numbers. The red arrow shows the approximate distance of the 1st hydration shell. (b) Coordination numbers of water around different functional group atoms connected to different benzene ring units, including the carboxylate C atom, the amide N atom, the amide C atom, and the amine N atom, respectively. (For interpretation of the references to color in this figure legend, the reader is referred to the Web version of this article.)

coordination numbers of water molecules around the carbon atoms in each type of benzene units in the polyamide chain. For type 1 and 2 benzene units, the water coordination number on average around the benzene C atom within the first hydration shell (~4 Å distance) varies from 4 to 4.5, while those for type 3, 4 and 5 benzene units are only about 2.5. Thus, hydrophobic attraction between the M alginate monomer and type 3, 4, and 5 benzene ring units is thermodynamically more favorable. Moreover, the relative hydrophilicity/hydrophobicity of specific benzene ring unit is also related to the connected functional groups. In Fig. 10b we show variations of the coordination number of water oxygen around the characteristic atomic groups directly connected to each type of benzene ring units, including the carboxylate C atom, the amide N atom, the amide C atom, and the amine N atom, respectively. It is seen that water molecules could form more compact

hydration structures around the charged carboxylate groups, and less compact hydration structures around the amide groups, leading to more hydrophobicity of the type 3 and 4 benzene units than the type 1 and 2 counterparts. This is consistent with the results shown in Fig. 10a.

In Fig. 8 we have also calculated the free energy curves of the ionic bridge binding between alginate monomers and different polyamide benzene ring units in the presence of divalent Ca^{2+} ions in a 0.1 M $CaCl_2$ solution. Such type of ionic bridge binding has been extensively studied in our previous work [30,31,70] and only occurs for type 1 and 2 benzene units which contain one or two polyamide carboxylate groups (Fig. 7). As we find the free energy curves of ionic bridge binding are almost the same for type 1 and 2 benzene units, only one curve is shown in Fig. 8. Here, the free energy profile for both M and G monomers interacting with polyamide carboxylate group exhibits a first free energy

minimum at about 4.3 Å, followed by a wide second energy minimum between 5.2-6.7 Å molecular distance. The energy barrier between the two minima is about 6 kcal/mol. The first energy minimum corresponds to the bidentate ionic bridge or the contact ionic pair (CIP) conformation, in which four oxygen atoms from the two carboxylate groups (one from the alginate monomer and the other from the polyamide benzene ring units of type 1 or 2) and four water molecules form the first hydration shell around the Ca²⁺ ion (Fig. 11a). The second broader energy minimum corresponds to the solvent-shared ionic pair (SSIP) conformation, in which the Ca²⁺ ion is coordinated with five water molecules in the first hydration shell (two of them have association with the carboxylate group in alginate monomer), together with two oxygen atoms from the carboxylate group of the polyamide (Fig. 11b). The bidentate CIP conformation is energetically more favorable than the SSIP conformation with a further free energy decrease by about 2 kcal/mol, as shown by the red dashed lines in Fig. 8. Dissociation of the SSIP conformation requires to overcome the last free energy barrier close to 2 kcal/mol at about 6.7 Å distance.

3.2. Mobility of individual M alginate monomers on surface polyamide chains

The moderately strong hydrophobic interactions between individual M alginate monomers and type 3, 4, and 5 benzene units in polyamide chains (Fig. 8a) result in an interesting phenomenon: the foulant monomers have the ability to "slide" along the membrane surface chains until they occasionally meet type 1 or 2 benzene rings to leave the chain surface. This is clearly shown in Fig. 9a-d, and in the supplemental movie (see the Supplemental Information). Such a mobility of the M monomer on the chain surface is quite different from the ionic bridge binding in which the alginate monomer is almost "permanently" bound to the carboxylate group of the chain surface through Ca²⁺ ion (Fig. 9e). Further free energy calculations along the backbone of the polyamide chain surface are performed, yielding a free energy profile along the lateral sliding direction shown in Fig. 9f. Here, the sliding distance s starts from the equilibrium conformation between the M monomer and type 5 benzene unit (Fig. 9a) (set as s = 0). The first free energy minimum in the purple segment corresponds to the metastable conformation in which the hydrophobic side of the M alginate monomer stays in close contact with the type 5 benzene ring surface. This energy minimum has the same value of 2.2 kcal/mol for the unbinding between the M monomer and type 5 benzene ring unit (see Fig. 8a). Increasing the distance s towards type 4 benzene unit needs to overcome the first energy barrier of \sim 0.75 kcal/mol. This is for the monomer to pass through the amide group between types 5 and 4 benzene rings. Such an energy barrier is comparable to kT (~0.6 kcal/mol at room temperature), suggesting that the M alginate monomer can easily move between the two types of hydrophobic benzene units (a - b in Fig. 9f). The free energy curve for the M monomer to move between types 4 to 3 benzene units shows the similar energy barrier (b - c in Fig. 9f). However, moving from type 3 to type 2 benzene unit needs to overcome a much higher energy barrier (~1.5 kcal/mol, see c - d segment in Fig. 9f). This scenario occurs

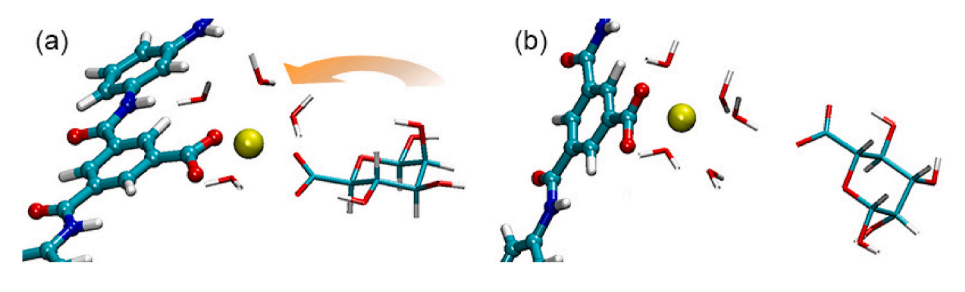
when the carboxylate group associated with the type 2 benzene unit has no bound Ca²⁺ ion. Thus, the hydrophobic interaction between the M monomer and type 2 benzene ring unit is highly unfavorable (Fig. 9d). In a very different scenario, if the carboxylate group associated with the type 2 benzene unit is already bound to a Ca²⁺ ion, then there is a very high probability that the ionic bridge between the M alginate monomer and the polyamide chain will form through the carboxylate(M)-Ca²⁺carboxylate(connected to type 2 benzene unit) complex in the CIP conformation (Fig. 11a). This situation can easily occur if the foulant monomer adopts a favorable orientation towards the ionic binding site right after the detachment from the polyamide backbone (see Figs. 9d and 11a). The same scenario could happen for the M monomer bound to the Ca^{2+} -carboxylate complex associated with type 1 benzene unit. Given the complex pathway for the M alginate monomer to form an ionic bridge with a surface polyamide chain, we anticipate that a single collective variable such as the distance s along the polyamide backbone is not sufficient to give a complete free energy surface of the foulantpolyamide chain interactions. However, our free energy calculations for the M alginate monomer sliding along the polyamide backbone shows that the moderately strong hydrophobic interactions between the monomer and different polyamide benzene ring units significantly decrease the docking time of the M monomer on the polyamide membrane surface. This is in contrast to the G monomer which has a much longer docking time on the membrane surface than the M monomers (see discussions in the next section).

3.3. Fouling behaviors of different alginate oligomers on a polyamide surface

We now consider the fouling behaviors of different alginate oligomers on a specifically designed polyamide model surface. Given the fact that oligomers containing mixed M and G monomers exhibit the similar fouling behavior, in this section we mainly focus on the studies of M-G-M and pure G-G-G/M-M-M oligomers.

To understand the general fouling mechanisms of these three different alginate oligomers on a representative polyamide surface, we build a specific membrane surface using our hybrid method (section 2). On this surface, more negatively charged functional groups are distributed in the left region of the membrane surface and the right region of the surface is largely kept neutral. The surface density of carboxylate groups on the left part is around 0.8 M. Fig. 12 shows the electrostatic potential distribution of the polyamide surface. The blue and red regions correspond to the neutral and negatively charged surface potentials, respectively.

Upon the membrane surface is fully hydrated, the three representative oligomers are introduced into the solution system. The initial distance between the center of mass of alginate oligomers and polyamide surface is set to $\sim\!25$ Å. Following the same procedure used in our previous studies [30,31], we use a drag-and-release approach to position oligomers near five different sites on the polyamide surface. These sites are selected based on a simple even distribution rule: two in the negatively charged region (triangle shape), two in the neutral region (oval



tact ionic pair (CIP) binding conformation and (b) the solvent-shared ionic pair (SSIP) binding conformation between an alginate monomer and a carboxylate group of a surface polyamide chain. The free energy minima corresponding to (a) and (b) are located at about 4.3 Å and 5.2–6.7 Å, respectively (see the red dashed lines in Fig. 8). The orange arrow in (a) shows the favorable approaching direction for the alginate to form ionic bridge binding. Colors: red, O; white, H; light blue, C; dark blue, N; yellow, Ca²⁺ ion. (For interpretation of the

Fig. 11. (a) The bidentate ionic bridge or the con-

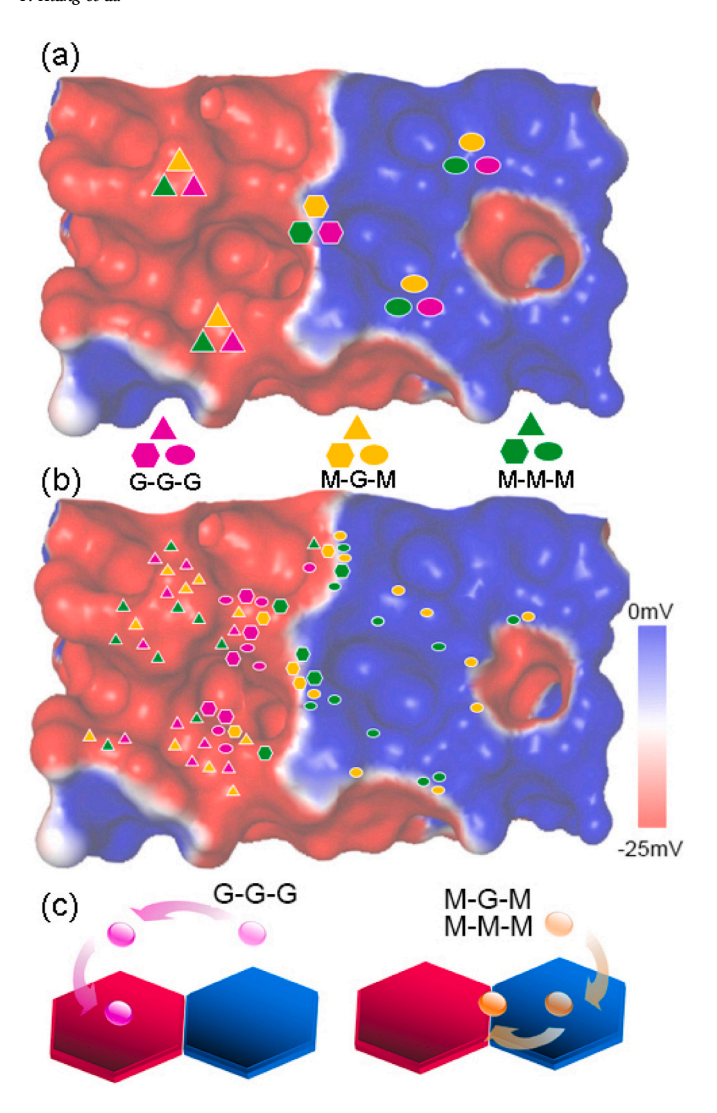


Fig. 12. (a) The start positions and (b) the final docking positions of alginate oligomers on the polyamide surface. Different colors indicate different types of alginate oligomers. The triangle, oval and hexagon shapes represent the alginates starting from the negatively charged surface, neutral surface, and boundary between the two, respectively. The colors of the polyamide surface show electrostatic potential distributions (represented by a van der Waals surface). (c) Schematics of the docking procedures for the G-G-G and M-G-M/M-M-M alginate oligomers with the start positions above the neutral side of the membrane surface. (For interpretation of the references to color in this figure legend, the reader is referred to the Web version of this article.)

shape), and one located at the boundary between the two regions (hexagon shape) (Fig. 12a). The drag-and-release approach is realized by applying a small dragging force (0.1–0.3 nN) to the oligomer to pull the molecule towards the five different sites. When the distance between the nearest oligomer-polyamide atom pair is within 5 Å, the dragging force is removed and then release the alginate molecule. Usually, the alginate oligomer could be docked on the polyamide surface. The system is equilibrated for at least 10 ns to find the final docking position of the oligomer. On each site, five independent simulation runs are performed for each oligomer, resulting in a total of 75 equilibrium simulation runs.

Fig. 12b summarize the final docking positions of the three alginate oligomers. It is seen that the G-G-G oligomers (pink symbols) *only* deposit on the negatively charged region through ionic bridge binding with the exposed carboxylate groups on the polyamide surface. We find that a total of seven out of ten G-G-G oligomers from the neutral region (pink oval symbols) migrate to the red negatively charged region, while the other three samples still stay in the solution during the simulation runs.

Further trajectory analysis reveals that the seven G-G-G oligomers from the neutral region drift a long distance in the solution to the negatively charged region (see Fig. 12c, left panel). Once the ionic bridges are formed, these oligomers can only slightly move around the binding sites, indicating that the binding strength of ionic bridge is rather strong.

The M-G-M and M-M-M oligomers originally released above the negatively charged region (yellow and green triangles in Fig. 12a) can directly form ionic bridges with polyamide carboxylate groups on the surface, similar to the fouling behavior of G-G-G oligomers released in the same region. However, the M-G-M and M-M-M oligomers released above the neutral region and near the boundary between the two regions (yellow and green ovals/hexagons) exhibit very different migration behaviors. In general, these M-G-M and M-M-M oligomers first attach to the neutral membrane surface through hydrophobic interactions. They then slowly migrate (slide) towards the negatively charged surface to form strong ionic bridges with polyamide carboxylate groups on the surface (see Fig. 12c, right panel). Consequently, most M-G-M and M-M-M oligomers are finally docked near the boundary between the negatively charged and neutral regions. If we consider that the whole membrane surface could be roughly divided into two regions according to fouling status, namely the severe fouling region on the left and the mild fouling region on the right, then such a chemical heterogeneity of polyamide membrane surface corroborates what has been measured in atomic force microscopy (AFM) experiments by Kim et al. [71], who concluded that the membrane surface with higher chemical heterogeneity (more concentrated binding sites in larger region) was more prone to fouling, suggesting that surface charge distribution is one of the key factors governing polyamide membrane fouling. In our model, although there is a small negatively charged patch on the right mild fouling region (Fig. 12a and b), it has a much less fouling potential than the left severe fouling region. These findings are consistent with the AFM experimental results.

Although on average the docking times for the three different oligomers released above the negatively charged membrane surface are roughly the same (i.e., \sim 5 ns for G-G-G and \sim 4.5 ns for M-G-M and M-M-M), the docking times of the oligomers released above the neutral region are quite different. We find that for G-G-G it takes about 8.5 ns to form an ionic bridge on the polyamide surface, while for M-G-M and M-M-M oligomers it takes about 1.5 ns to induce a hydrophobic attachment on the surface first, followed by another ~ 2.5 ns to form ionic bridge binding in most cases. Such different docking times and pathways between the G-G-G and M-G-M/M-M-M oligomers (Fig. 12c) show that hydrophobic interactions between the M-contained alginate foulant and polyamide surface enhance the surface fouling. It is interesting to see that the more stable ionic bridge binding is formed more slowly than the relatively weak hydrophobic attachment. Such phenomenon could be attributed to two reasons. First, ionic bridge binding requires that the binding sites (carboxylate groups on the polyamide surface) are preoccupied by metal ions before the arrival of the foulant, while the hydrophobic attraction only requires the presence of the type 3, 4 or 5 benzene units on the membrane surface. And second, there are usually more hydrophobic benzene units than carboxylate groups on the polyamide membrane surface (the ratio is more than 5:1). As such, the number of effective binding sites on the membrane surface for hydrophobic attraction is much higher than that for ionic bridge binding, resulting in much less docking time for hydrophobic attachment.

The finding here may imply a general fouling mechanism for alginate polymers containing M monomers: Initially the foulant deposits on the membrane surface through hydrophobic interactions, which could be considered as a *kinetic* process with moderate binding strength. Upon the hydrophobic attachment the foulant still has some mobility on the membrane surface to search for the most stable binding sites with the lowest free energy state (ionic bridge). This later process could be considered as a *thermodynamic* process. Because hydrophobic interactions between M monomers and polyamide surface can significantly reduce the time required to form subsequent ionic bridge binding,

we conclude that this moderately strong hydrophobic attraction may promote the ionic bridge binding by keeping the relevant polyamide carboxylate functional groups in the vicinity of the alginate foulant (Fig. 9d and e).

4. Conclusions

In this study, we perform molecular dynamics and free energy simulations to investigate the interactions between polyamide membrane surface and alginate molecules. A hybrid method has been used to build cross-linked polyamide membrane, which could control the composition and functional group density on the membrane surface. Free energy calculations for the G and M alginate monomers interacting with different types of benzene ring units on the polyamide surface show the moderately strong hydrophobic attraction between the amphiphilic M monomer and types 3–5 benzene ring units. This hydrophobic interaction, however, does not exist between the G monomer and polyamide surface chains.

Though the hydrophobic attraction between the M monomer in an alginate oligomer and polyamide surface chains is not as strong as the ionic bridge binding, it nevertheless plays an important role in enhancing the ionic bridge binding by keeping the relevant functional groups in both polyamide and alginate in the vicinity. The present study provides valuable insights into the fouling mechanism of polyamide membranes by alginates and the findings may help to understand the general fouling mechanism by other organic foulants.

Author statement

Yuan Xiang: Conceptualization, Methodology, Software, Validation, Formal analysis, Data curation, Visualization, Writing – original draft. Rong-guang Xu: Conceptualization, Methodology, Software. Yongsheng Leng: Conceptualization, Methodology, Writing – review & editing, Supervision, Project administration, Funding acquisition.

Declaration of competing interest

The authors declare that they have no known competing financial interests or personal relationships that could have appeared to influence the work reported in this paper.

Acknowledgements

This work was supported by the National Science Foundation (NSF 1817394) and the resources of the National Energy Research Scientific Computing Center (NERSC), a DOE Office of Science User Facility supported by the Office of Science of the U.S. Department of Energy under Contract no. DE-AC02-05CH11231.

Appendix A. _Supplementary data

Supplementary data related to this article can be found at https://doi.org/10.1016/j.memsci.2021.120078.

References

- K.C. Khulbe, C. Feng, T. Matsuura, The art of surface modification of synthetic polymeric membranes, J. Appl. Polym. Sci. 115 (2010) 855–895.
- [2] L.M. Camacho, L. Dumee, J. Zhang, J.-d. Li, M. Duke, J. Gomez, S. Gray, Advances in membrane distillation for water desalination and purification applications, Water 5 (2013) 94–196.
- [3] S. Zhao, L. Zou, C.Y. Tang, D. Mulcahy, Recent developments in forward osmosis: opportunities and challenges, J. Membr. Sci. 396 (2012) 1–21.
- [4] M. Elimelech, W.A. Phillip, The future of seawater desalination: energy, technology, and the environment, Science 333 (2011) 712–717.
- [5] G.-d. Kang, Y.-m. Cao, Development of antifouling reverse osmosis membranes for water treatment: a review, Water Res. 46 (2012) 584–600.
- [6] W.J. Lau, A.F. Ismail, N. Misdan, M.A. Kassim, A recent progress in thin film composite membrane: a review, Desalination 287 (2012) 190–199.

- [7] A. Perez-Gonzalez, A.M. Urtiaga, R. Ibanez, I. Ortiz, State of the art and review on the treatment technologies of water reverse osmosis concentrates, Water Res. 46 (2012) 267–283.
- [8] K.P. Lee, T.C. Arnot, D. Mattia, A review of reverse osmosis membrane materials for desalination-Development to date and future potential, J. Membr. Sci. 370 (2011) 1–22.
- [9] C.Y. Tang, T.H. Chong, A.G. Fane, Colloidal interactions and fouling of NF and RO membranes: a review, Adv. Colloid Interface Sci. 164 (2011) 126–143.
- [10] D. Rana, T. Matsuura, Surface modifications for antifouling membranes, Chem Rev. 110 (2010) 2448–2471.
- [11] J. Brant, A. Childress, Membrane-colloid interactions: comparison of extended DLVO predictions with AFM force measurements, Environ. Eng. Sci. 19 (2002) 413-427
- [12] X. Jin, X. Huang, E. Hoek, Role of specific ion interactions in seawater RO membrane fouling by alginic acid, Environ. Sci. Technol. 43 (2009) 3580–3587.
- [13] M. Elimelech, X.H. Zhu, A.E. Childress, S.K. Hong, Role of membrane surface morphology in colloidal fouling of cellulose acetate and composite aromatic polyamide reverse osmosis membranes, J. Membr. Sci. 127 (1997) 101–109.
- [14] T. Wei, L. Zhang, H.Y. Zhao, H. Ma, M.S.J. Sajib, H. Jiang, S. Murad, Aromatic polyamide reverse-osmosis membrane: an atomistic molecular dynamics simulation, J. Phys. Chem. B 120 (2016) 10311–10318.
- [15] W.-F. Chan, H.-y. Chen, A. Surapathi, M.G. Taylor, X. Hao, E. Marand, J. K. Johnson, Zwitterion functionalized carbon nanotube/polyamide nanocomposite membranes for water desalination, ACS Nano 7 (2013) 5308–5319.
- [16] Y.-x. Shen, W. Si, M. Erbakan, K. Decker, R. De Zorzi, P.O. Saboe, Y.J. Kang, S. Majd, P.J. Butler, T. Walz, A. Aksimentiev, J.-l. Houb, M. Kumar, Highly permeable artificial water channels that can self-assemble into two-dimensional arrays, Proc. Natl. Acad. Sci. U. S. A 112 (2015) 9810–9815.
- [17] L.-C. Lin, J.C. Grossman, Atomistic understandings of reduced graphene oxide as an ultrathin-film nanoporous membrane for separations, Nat. Commun. 6 (2015), 8335-8335.
- [18] C. Zhu, H. Li, S. Meng, Transport behavior of water molecules through twodimensional nanopores, J. Chem. Phys. 141 (2014).
- [19] J.-G. Gai, X.-L. Gong, W.-L. Kang, X. Zhang, W.-W. Wang, Key factors influencing water diffusion in aromatic PA membrane: hydrates, nanochannels and functional groups, Desalination 333 (2014) 52–58.
- [20] V. Kolev, V. Freger, Hydration, porosity and water dynamics in the polyamide layer of reverse osmosis membranes: a molecular dynamics study, Polymer 55 (2014) 1420–1426.
- [21] D. Cohen-Tanugi, J.C. Grossman, Water desalination across nanoporous graphene, Nano Lett. 12 (2012) 3602–3608.
- [22] Y. Liu, X. Chen, High permeability and salt rejection reverse osmosis by a zeolite nano-membrane, Phys. Chem. Chem. Phys. 15 (2013) 6817–6824.
- [23] Z. Hu, Y. Chen, J. Jiang, Zeolitic imidazolate framework-8 as a reverse osmosis membrane for water desalination: insight from molecular simulation, J. Chem. Phys. 134 (2011).
- [24] I. Davis, B. Shachar-Hill, M. Curry, K. Kim, T. Pedley, A. Hill, Osmosis in semi-permeable pores: an examination of the basic flow equations based on an experimental and molecular dynamics study, Proc. Roy. Soc. A 463 (2007) 881–896.
- [25] W. Jia, S. Murad, Molecular dynamics simulation of pervaporation in zeolite membranes, Mol. Phys. 104 (2006) 3033–3043.
- [26] K. Kim, I. Davis, P. Macpherson, T. Pedley, A. Hill, Osmosis in small pores: a molecular dynamics study of the mechanism of solvent transport, Proc. Roy. Soc. Lond. A Math. 461 (2005) 273–296.
- [27] S. Murad, L. Nitsche, The effect of thickness, pore size and structure of a nanomembrane on the flux and selectivity in reverse osmosis separations: a molecular dynamics study, Chem. Phys. Lett. 397 (2004) 211–215.
- [28] A. Raghunathan, N. Aluru, Molecular understanding of osmosis in semipermeable membranes, Phys. Rev. Lett. 97 (2006), 024501.
- [29] W. Ahn, A. Kalinichev, M. Clark, Effects of background cations on the fouling of polyethersulfone membranes by natural organic matter: experimental and molecular modeling study, J. Membr. Sci. 309 (2008) 128–140.
- [30] Y. Xiang, Y.L. Liu, B.X. Mi, Y.S. Leng, Hydrated polyamide membrane and its interaction with alginate: a molecular dynamics study, Langmuir 29 (2013) 11600–11608.
- [31] Y. Xiang, Y.L. Liu, B.X. Mi, Y.S. Leng, Molecular dynamics simulations of polyamide membrane, calcium alginate gel, and their interactions in aqueous solution, Langmuir 30 (2014) 9098–9106.
- [32] Z.E. Hughes, J.D. Gale, Molecular dynamics simulations of the interactions of potential foulant molecules and a reverse osmosis membrane, J. Mater. Chem. 22 (2012) 175–184.
- [33] H. Eslami, F. Muller-Plathe, Molecular dynamics simulation of water influence on local structure of nanoconfined polyamide-6,6, J. Phys. Chem. B 115 (2011) 9720–9731.
- [34] E. Harder, D.E. Walters, Y.D. Bodnar, R.S. Faibish, B. Roux, Molecular dynamics study of a polymeric reverse osmosis membrane, J. Phys. Chem. B 113 (2009) 10177–10182.
- [35] Z.E. Hughes, J.D. Gale, A computational investigation of the properties of a reverse osmosis membrane, J. Mater. Chem. 20 (2010) 7788–7799.
- [36] M. Kotelyanskii, N.J. Wagner, M.E. Paulaitis, Building large amorphous polymer structures: atomistic simulation of glassy polystyrene, Macromolecules 29 (1996) 8497–8506.
- [37] M.J. Kotelyanskii, N.J. Wagner, M.E. Paulaitis, Atomistic simulation of water and salt transport in the reverse osmosis membrane FT-30, J. Membr. Sci. 139 (1998) 1–16

- [38] R. Nadler, S. Srebnik, Molecular simulation of polyamide synthesis by interfacial polymerization, J. Membr. Sci. 315 (2008) 100–105.
- [39] H.F. Ridgway, J.D. Gale, Z.E. Hughes, M.B. Stewart, J.D. Orbell, S.R. Gray, Functional Nanostructured Materials and Membranes for Water Treatment, Book News, Inc., Portland, 2013.
- [40] S. Lee, M. Elimelech, Relating organic fouling of reverse osmosis membranes to intermolecular adhesion forces, Environ. Sci. Technol. 40 (2006) 980–987.
- [41] B. Mi, M. Elimelech, Chemical and physical aspects of organic fouling of forward osmosis membranes, J. Membr. Sci. 320 (2008) 292–302.
- [42] Q.L. Li, Z.H. Xu, I. Pinnau, Fouling of reverse osmosis membranes by biopolymers in wastewater secondary effluent: role of membrane surface properties and initial permeate flux, J. Membr. Sci. 290 (2007) 173–181.
- [43] D. Nanda, K.L. Tung, Y.L. Li, N.J. Lin, C.J. Chuang, Effect of pH on membrane morphology, fouling potential, and filtration performance of nanofiltration membrane for water softening, J. Membr. Sci. 349 (2010) 411–420.
- [44] T.D. Perry, R.T. Cygan, R. Mitchell, Molecular models of alginic acid: interactions with calcium ions and calcite surfaces, Geochem. Cosmochim. Acta 70 (2006)
- [45] W. Plazinski, W. Rudzinski, Molecular modeling of Ca2+-oligo(alpha-l-guluronate) complexes: toward the understanding of the junction zone structure in calcium alginate gels, Struct. Chem. 23 (2012) 1409–1415.
- [46] J. Smith, Organic Chemistry, sixth ed., McGraw-Hill Education, New York, 2020.
- [47] Y. Xiang, R.G. Xu, Y.S. Leng, Molecular dynamics simulations of a poly(ethylene glycol)-grafted polyamide membrane and its interaction with a calcium alginate gel, Langmuir 32 (2016) 4424–4433.
- [48] X.J. Zhang, D.G. Cahill, O. Coronell, B.J. Marinas, Absorption of water in the active layer of reverse osmosis membranes, J. Membr. Sci. 331 (2009) 143–151.
- [49] B.X. Mi, D.G. Cahill, B.J. Marinas, Physico-chemical integrity of nanofiltration/ reverse osmosis membranes during characterization by Rutherford backscattering spectrometry, J. Membr. Sci. 291 (2007) 77–85.
- [50] H.C. Flemming, H.F. Ridgway, Marine and Industrial Biofouling, Springer-Verlag, Berlin, 2009, pp. 103–117.
- [51] O. Coronell, M.I. Gonzalez, B.J. Marinas, D.G. Cahill, Ionization behavior, stoichiometry of association, and accessibility of functional groups in the active layers of reverse osmosis and nanofiltration membranes, Environ. Sci. Technol. 44 (2010) 6808–6814.
- [52] O. Coronell, B.J. Marinas, X. Zhang, D.G. Cahill, Quantification of functional groups and modeling of their ionization behavior in the active layer of FT30 reverse osmosis membrane, Environ. Sci. Technol. 42 (2008) 5260–5266.
- [53] Y.S. Leng, Hydration force between mica surfaces in aqueous KCl electrolyte solution, Langmuir 28 (2012) 5339–5349.
- [54] Y.S. Leng, Hydration force and dynamic squeeze-out of hydration water under subnanometer confinement, J. Phys.-Condes. Matter 20 (2008) 354017–354024.

- [55] K.P. Ishida, R.M. Bold, D.W. Phipps, Identification and Evaluation of Unique Chemicals for Optimum Membrane Compatibility and Improved Cleaning Efficiency, California department of water resources, 2005.
- [56] T.A. Davis, B. Volesky, A. Mucci, A review of the biochemistry of heavy metal biosorption by brown algae, Water Res. 37 (2003) 4311–4330.
- [57] T. Brown, H. Eugene H LeMay, B. Bursten, C. Murphy, P. Woodward, Chemistry: the Central Science, Prentice Hall, Boston, 2011.
- [58] S. Plimpton, Fast parallel algorithms for short range molecular dynamics, J. Comput. Phys. 117 (1995) 1–19.
- [59] R.W. Hockney, J.W. Eastwood, Computer Simulation Using Particles, Taylor and Francis Group, London, U.K., 1988.
- [60] M.P. Allen, D.J. Tildesley, Computer Simulation of Liquids, Clarendon Press, Oxford, 1987.
- [61] D.H. Kitson, A.T. Hagler, Theoretical studies of the structure and molecular dynamics of a peptide crystal, Biochemistry 27 (1988) 5246–5257.
- [62] C.M. Breneman, K.B. Wiberg, Determining atom-centered monopoles from molecular electrostatic potentials - the need for high sampling density in formamide conformational-analysis, J. Comput. Chem. 11 (1990) 361–373.
- [63] W.L. Jorgensen, D.S. Maxwell, J. TiradoRives, Development and testing of the OPLS all-atom force field on conformational energetics and properties of organic liquids, J. Am. Chem. Soc. 118 (1996) 11225–11236.
- [64] G.A. Kaminski, R.A. Friesner, J. Tirado-Rives, W.L. Jorgensen, Evaluation and reparametrization of the OPLS-AA force field for proteins via comparison with accurate quantum chemical calculations on peptides, J. Phys. Chem. B 105 (2001) 6474–6487.
- [65] J. Aqvist, Ion water interaction potentials derived from free-energy perturbation simulations, J. Phys. Chem. 94 (1990) 8021–8024.
- [66] I.S. Joung, T.E. Cheatham, Determination of alkali and halide monovalent ion parameters for use in explicitly solvated biomolecular simulations, J. Phys. Chem. B 112 (2008) 9020–9041.
- [67] S. Kumar, D. Bouzida, R.H. Swendsen, P.A. Kollman, J.M. Rosenberg, THE weighted histogram analysis method for free-energy calculations on biomolecules. I. The method, J. Comput. Chem. 13 (1992) 1011–1021.
- [68] G.M. Torrie, J.P. Valleau, Nonphysical sampling distributions in Monte Carlo freeenergy estimation: umbrella sampling, J. Comput. Phys. 23 (1977) 187–199.
- [69] M.B. Stewart, D.T. Myat, M. Kuiper, R.J. Manning, S.R. Gray, J.D. Orbell, A structural basis for the amphiphilic character of alginates-Implications for membrane fouling, Carbohydr. Polym. 164 (2017) 162–169.
- [70] Y. Xiang, R.G. Xu, Y.S. Leng, Molecular understanding of ion effect on polyzwitterion conformation in an aqueous environment, Langmuir 36 (2020) 7648–7657.
- [71] Y. Kim, S. Lee, J. Kuk, S. Hong, Surface chemical heterogeneity of polyamide RO membranes: measurements and implications. Desalination 367 (2015) 154–160.